

Journal of Materials Chemistry C

Accepted Manuscript



This is an *Accepted Manuscript*, which has been through the Royal Society of Chemistry peer review process and has been accepted for publication.

Accepted Manuscripts are published online shortly after acceptance, before technical editing, formatting and proof reading. Using this free service, authors can make their results available to the community, in citable form, before we publish the edited article. We will replace this *Accepted Manuscript* with the edited and formatted *Advance Article* as soon as it is available.

You can find more information about *Accepted Manuscripts* in the [Information for Authors](#).

Please note that technical editing may introduce minor changes to the text and/or graphics, which may alter content. The journal's standard [Terms & Conditions](#) and the [Ethical guidelines](#) still apply. In no event shall the Royal Society of Chemistry be held responsible for any errors or omissions in this *Accepted Manuscript* or any consequences arising from the use of any information it contains.

COMMUNICATION

Cite this DOI:
 10.1039/x0xx00000x
 Received 00th January
 2012,
 Accepted 00th January 2012
 DOI: 10.1039/x0xx00000x
 www.rsc.org/

Pyrene based materials for exceptionally deep blue OLEDs

Dennis Chercka,^a Seung-Jun Yoo,^b Martin Baumgarten,^a Jang-Joo Kim^{b‡} and Klaus Müllen^{a*}

A 2,7-functionalized pyrene-based emitter for highly efficient OLEDs has been developed. The chromophore can be prepared on a large scale in good yields. It offers an exceptional deep blue photoluminescence (CIE: $x = 0.16$, $y = 0.024$) and good external quantum efficiency (EQE) of 3.1 % when employed in a guest-host system OLED.

Less than thirty years after their inception as an academic field by the works of Tang et al. in 1987¹, organic light emitting diodes (OLEDs) have become a broadly applied commodity for display applications and, to a lesser degree, lighting applications². OLEDs are commonly used in display applications due to their low power consumption and good colour gamut.³ In full-colour devices red and green emission is provided by highly efficient phosphorescent transition metal complexes. In contrast, blue emission to this day often stems from fluorescent materials due to their better long-time stability. Deep blue electroluminescence allows the energy efficient enhancement of colour purity by strong microcavity structures.⁴

In this work we based the synthesis on pyrene. Its native deep blue fluorescence (in diluted solution) in combination with its high thermal and photostability make it attractive as a blue emitter. While having these desirable properties pyrene also has poor charge carrier mobility characteristics as well as a strong tendency for excimer formation.⁵ The pyrene–pyrene excimer has a significant bathochromic shift of the fluorescence of approx. 30–40 nm (a shift from “deep-blue” to “sky-blue” is the consequence).⁶ Thus, the design of pyrene derivatives used in OLED devices aims at disrupting pyrene–pyrene interactions. A simple yet efficient way to suppress excimer formation was reported in the form of tetra(o-tolyl)pyrene (TOTP).⁷ Poor external quantum efficiencies (EQE) in prepared OLEDs make this molecule more attractive as matrix (host) material. Several more sophisticated approaches have been discussed in the literature; for example poly-pyrenes prepared by an elegant 1-3-polymerization⁸ or pyrene core based poly-phenylene dendrimers.^{9,10} While providing excellent suppression of excimer formation and tuneable charge-carrier properties both classes of materials can only be processed from solution. Furthermore, they require significant synthetic efforts and complicated purification procedures. In a recent work by Kaafarani et al. a simple but efficient tert-butylcarbazole substituted pyrene derivative for a solution fabricated OLED has been reported.¹¹

For our study we designed a chromophore that can be processed from solution or by vapour deposition techniques and is easily prepared on a gram scale. The central element is a 2,7-functionalized pyrene scaffold. The 2- as well as the 7-position in pyrene have low orbital coefficients in both frontier orbitals resulting in weak conjugation to attached functional groups. This allows functionalization in these positions without compromising the large band gap behaviour of pyrene. The 3,6-ditertbutylcarbazole (**1**) moiety is connected to the pyrene scaffold by means of a meta-phenylene bridge. The bulky substituent is expected to hinder pyrene–pyrene excimer formation while enhancing the hole transport efficiency of the material.^{12,13} Molecular design also aimed at reducing the energy difference between the first excited singlet (S_1) and triplet state (T_1) to $\Delta E(S_1-T_1) < 0.5$ eV as suggested by Adachi.¹⁴ The T_1 states can be destabilized by orbital partitioning.¹⁵ The meta-phenylene bridge significantly increases the partitioning of the frontier orbitals compared to a para-arrangement (modelling results are shown in ESI). Tertiary-butyl groups are used to block the 3 and 6 positions in carbazole in order to improve the stability of the compound in the device and to increase the bulk of the substituents that hinder excimer formation.

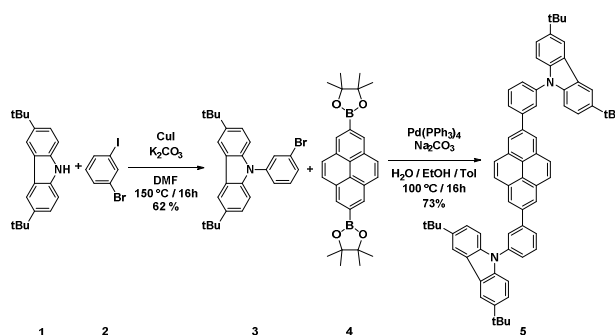


Figure 1 | Synthesis of compound 5.

For the synthesis of **5**, *N*-(2-bromophenyl)carbazole (**3**) is prepared by Ullmann-reaction catalysed by copper iodide in DMF. 2,7-Functionalized pyrenes are accessible by regio-selective iridium-catalysed C–H activation/borylation reaction.¹⁶ This key step of our synthetic strategy affords compound **4** in one step and high yields. The target compound **5** is obtained by subsequent Suzuki cross coupling reaction. This conversion is sensitive to the nature of the base used. **5** was obtained in low yield (36 %) and conversion remained incomplete when potassium carbonate was used as a base.¹⁷ An aqueous solution

of sodium carbonate ($c = 2 \text{ mol/l}$) gives full conversion as well as high yields of **5**. Due to low solubility of **5**, purification by column chromatography was not feasible. Repeated recrystallization from hexane afforded the clean product in 73 % yield (m.p.: 225 – 226 °C).

Frontier orbital energies (E_{HOMO} and E_{LUMO}) and the associated energy gap ΔE_{opt} were determined using the cyclic voltammogram and absorption spectrum of **5**. The results are summarized in table 1. As expected, it was only possible to resolve the oxidation signal at 1.57 V (vs SCE).¹⁸ Thus, E_{LUMO} was determined in conjunction with the optical band gap ΔE_{op} derived from the solution UV/Vis-spectrum. The value of theoretical band gap $\Delta E_{\text{(DFT)}}$ (DFT, B3LYP, 6-31G^{*}) is in good agreement with the experimental value. In contrast, the absolute values of the frontier orbital energies have a 0.6 eV discrepancy between the experimental and theoretical data. As DFT-calculations were performed in gas-phase only, solvent effects occurring during experimental characterization were not taken into account.

Table 1: Frontier orbital energies

E_{HOMO} (CV.) [eV]	ΔE (opt.) [eV]	E_{LUMO} (Exp.) [eV]	E_{HOMO} (DFT) [eV] ^a	ΔE (DFT) [eV] ^a	E_{LUMO} (DFT) [eV] ^a
-6.01	3.4	-2.6	-5.42	3.5	-1.98

^a DFT, B3LYP, 6-31G^{*}

Figure 2 shows the optical spectra of compound **5** in THF solution and in a thin film prepared by thermal evaporation on fused silica. The UV/Vis spectra are characterized by an absorption maximum at $\lambda_{\text{max,abs}} = 298 \text{ nm}$, while the onset is determined at $\lambda = 365 \text{ nm}$. Vibrational fine splitting is not resolved as previously reported for other 2,7-functionalized pyrene derivatives.¹⁹ Weaker absorption bands are observed at $\lambda = 244 \text{ nm}$, $\lambda = 348 \text{ nm}$ and $\lambda = 332 \text{ nm}$. A small bathochromic shift occurs in the solid state.

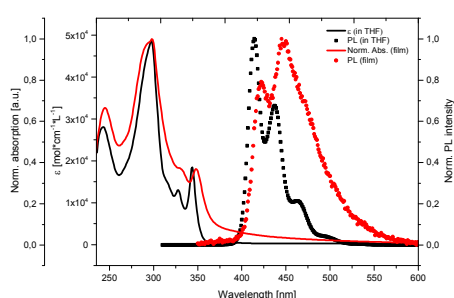


Figure 2 | Absorption and fluorescence spectra of **5** in THF solution (black) and in a thin film (red).

The solution fluorescence spectrum features three bands at $\lambda_{\text{max,PL}} = 414 \text{ nm}$, $\lambda_{\text{PL}} = 436 \text{ nm}$ and $\lambda_{\text{PL}} = 464 \text{ nm}$ and a FWHM of 39.7 nm. The thin film shows a structured emission with its maximum at $\lambda_{\text{max,PL}} = 447 \text{ nm}$ and a shoulder at $\lambda = 421 \text{ nm}$. The compound exhibits a pronounced Stokes-shift by almost 50 nm, which is characteristic for a large reorganization in the excited state.⁶ Large Stokes shifts are common for 2,7-pyrenes.^{11,20} Concentration dependent emission spectra are shown in the ESI (S3). The transition at $\lambda_{\text{PL}} = 438 \text{ nm}$ gains in intensity at higher

concentrations, i.e. as aggregation becomes favourable. The emission of **5** is virtually independent of the solvent polarity (ESI, S4) suggesting a small transition dipole moment.²¹ In poor solvents (e.g. hexane) the 438 nm band is more intense as aggregation is strong.

It was considered to prepare OLEDs with a doped matrix emissive layer (EL), using mCPPO1 (9-(3-(9H-carbazole-9-yl)phenyl)-3-(dibromophenylphosphoryl)-9H-carbazole) as matrix material and **5** as fluorescent dopant.²² A series of films (5 wt% and 10 wt% **5** in mCPPO1; mCPPO1:**5**) was prepared (figure 3). It is noteworthy that a significant hypsochromic shift of fluorescence is observed for the doped films. The weaker signal in the neat film of **5** ($\lambda = 420 \text{ nm}$) develops into a sharp fluorescence maximum at $\lambda_{\text{max,PL}} = 415 \text{ nm}$ (shifted by 5 nm). At the same time the fluorescence maximum at $\lambda = 447 \text{ nm}$ is diminished to a weak shoulder at $\lambda = 437 \text{ nm}$ (shifted by 10 nm). The FWHM of the doped films' fluorescence is only 43 (± 1) nm compared to the 70 (± 1) nm of neat film. In essence, the solution PL spectrum is (slightly broadened) re-established. The PL efficiency of a neat film of **5** was determined by the integrating sphere method to 47 %. When **5** was doped into the mCPPO1 matrix material the value dropped to 41 % (10 wt.% of **5**) and 37 % (5 wt.% of **5**).

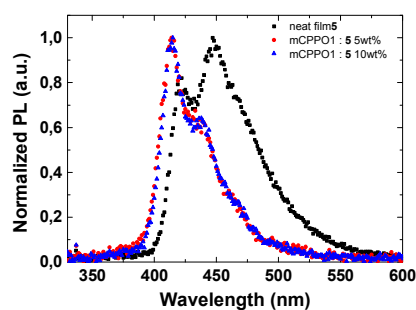


Figure 3 | PL Spectra of thin-films prepared by vapour deposition (**5**, black squares; 5 wt% of **5** in mCPPO1, red dots; 10 wt% in mCPPO1, blue triangles)

The pure film of **5** showed a bathochromic shift in the absorption and emission spectra (compared to the solution data) due to intermolecular interaction (i.e. aggregation). As a result of the chromophore design, however, an excimer formation is prevented. When the compound is embedded into a matrix of mCPPO1 the single molecule fluorescence is established. The low emitter concentration in the film probably suppresses aggregation. From this we concluded that a guest-host structure emitting layer (EL) would be more promising for deep blue OLEDs and was used hence forth.

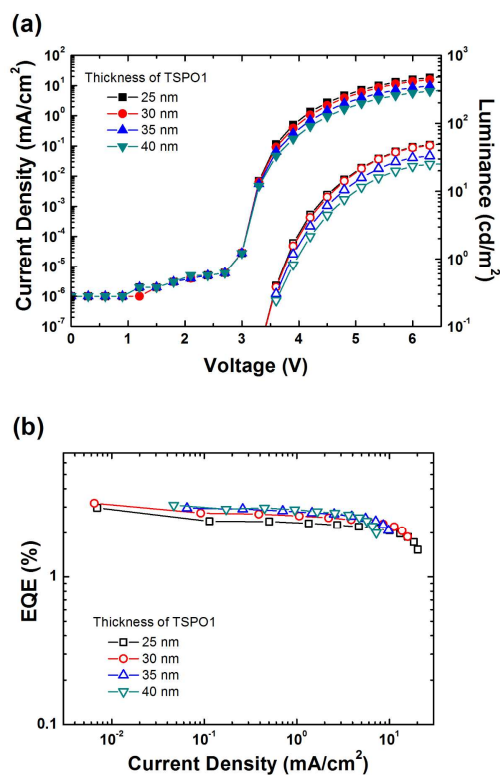


Figure 4 | (a) The current density-voltage-luminance curve and (b) quantum efficiency-current density of OLEDs with varying the thickness of TSPO1.

OLEDs were fabricated by thermal evaporation. The device structure was as follows (an illustration is available in the ESI): glass/ITO (150 nm)/ReO₃ (1 nm)/mCP (25 nm)/mCPPO1 (10 nm)/mCPPO1:5 5 wt% (30 nm)/TSPO1 (25,30,35,40 nm)/LiF (0.7 nm)/Al (100 nm).²³

mCP (*N,N'*-dicarbazolyl-3,5-benzene) was used as hole transport material (HTL), and TSPO1 (diphenylphosphine oxide-4-(triphenylsilyl)phenyl) as electron transport material (ETL). The mCPPO1:5 guest-host system was chosen as EL and prepared by co-deposition. The hole injection barrier between ITO and mCP ($E_{\text{HOMO}} = -6.1$ eV) was reduced by using a thin ReO₃ layer.²⁴ mCPPO1 was chosen as additional blocking layer and TSPO1 as an electron transport layer, as their triplet energy exceeds the triplet energy of **5**.²² Thus, the energy transfer from the triplet state of **5** to the host-/ charge carrier transport materials is prevented (illustrated in ESI) and this loss-channel closed.

The current density-voltage-luminance (*J-V-L*) characteristics of the OLEDs are given in Figure 4(a). The device performance of the OLEDs is summarized in table 2. Turn-on voltages (at 0.1 cd/m²) of the OLEDs are 3.4 V regardless of TSPO1 thickness. Figure 4(b) illustrates the quantum efficiency-current density of OLEDs. The maximum EQE of 3.19 % was obtained from the device with 30 nm thickness of TSPO1.

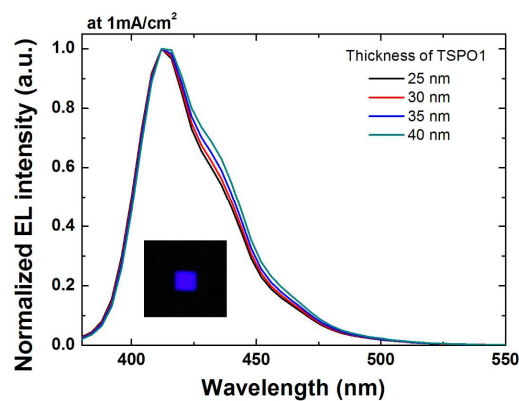


Figure 5 | Normalized EL spectra of OLEDs at 1 mA/cm² with varying ETL thicknesses.

The electroluminescent (EL) spectra at 1 mA/cm² with varying ETL thicknesses are given in figure 5. The EL emission peak of the OLEDs ranges from 390 – 475 nm with the maximum (EL_{max}) located at 412 nm regardless of the thickness of TSPO1. As expected, the EL spectrum is similar to the PL spectrum of mCPPO1:5 5wt % film. With increasing ETL thickness a weak shoulder arises at 430 nm due to cavity effects. The combination of material **5** and optimized device structure results in exceptional spectral purity, the *Commission Internationale de l'Eclairage 1931* (CIE1931) coordinates of OLEDs at 1 mA/cm² are $x = 0.16$, $y = 0.024$ regardless of the thickness of TSPO1. To our best knowledge, this colour purity is the deepest in blue OLEDs so far reported in literature. OLEDs using **5** as “emitter-only” EML were prepared as reference devices (see ESI S9 for details).

Table 2 | Summary of device performance in correlation with ETL thickness.

ETL thickness [nm]	$V_{\text{turn-on}}^a$ [V]	EQE_{max}^b [%]	EQE^c [%]	EL_{max}^c [nm]	CIE ^c (x, y)
25	3.4	2.97	2.34	412	(0.16, 0.024)
30	3.4	3.19	2.62	412	(0.16, 0.024)
35	3.4	2.95	2.78	412	(0.16, 0.024)
40	3.4	3.09	2.87	412	(0.16, 0.024)

^a Turn-on voltage at 0.1 cd/m² ^b Maximum EQE ^c At 1 mA/cm²

Conclusions

We have presented a new pyrene based emitter material (**5**) for OLED devices. The hole transport properties of pyrene are enhanced while excimer formation is prevented by incorporating N-phenylene-carbazole-pendant units in position 2 and 7. In guest-host systems of mCPPO1:5 (prepared by co-evaporation) the single molecule emission of **5** is established. When this system is employed in optimized OLED devices an exceptionally deep EL colour purity (CIE: $x = 0.16$, $y = 0.024$) and good EQE values (3.1 %) are observed.

Notes and references

^a Max Planck Institute for Polymer Research
Ackermannweg 10, 55128 Mainz, Germany.

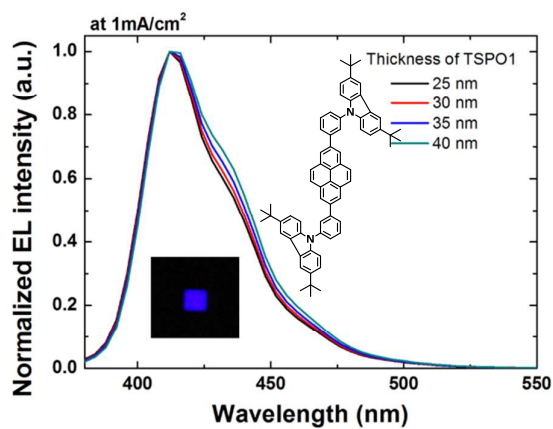
[†]Mueller@mpip-mainz.mpg.de

^b Seoul National University,
Seoul, 151-744, Republic of Korea.

[‡]JJKim@snu.ac.kr

Electronic Supplementary Information (ESI) available: [Experimental procedures, NMR-, solution UV/Vis spectra, molecular modelling as well as CV data and device structure]. See DOI: 10.1039/c000000x/

1. C. W. Tang and S. A. VanSlyke, *Appl. Phys. Lett.*, 1987, **51**, 913-915.
2. N. Thejo Kalyani and S. J. Dhoble, *Renew. Sust. Energ. Rev.*, 2012, **16**, 2696-2723.
3. L. E. Germany, www.presse.lge.de, 2013.
4. S. Chen, L. Deng, J. Xie, L. Peng, L. Xie, Q. Fan and W. Huang, *Adv. Mater.*, 2010, **22**, 5227-5239.
5. T. M. Figueira-Duarte and K. Müllen, *Chem. Rev.*, 2011, **111**, 7260-7314.
6. J. B. Birks and L. G. Christophorou, *Spectrochim. Acta*, 1963, **19**, 401-410.
7. C.-C. Yeh, M.-T. Lee, H.-H. Chen and C. H. Chen, *SID Symposium Digest of Technical Papers*, 2004, **35**, 788-791.
8. R. Trattnig, T. M. Figueira-Duarte, D. Lorbach, W. Wiedemair, S. Sax, S. Winkler, A. Vollmer, N. Koch, M. Manca, M. A. Loi, M. Baumgarten, E. J. W. List and K. Müllen, *Opt. Express*, 2011, **19**, A1281-A1293.
9. S. Bernhardt, M. Kastler, V. Enkelmann, M. Baumgarten and K. Müllen, *Chem. Eur. J.*, 2006, **12**, 6117-6128.
10. J. You, G. Li, R. Wang, Q. Nie, Z. Wang and J. Li, *PCCP*, 2011, **13**, 17825-17830.
11. B. R. Kaafarani, A. O. El-Ballouli, R. Trattnig, A. Fonari, S. Sax, B. Wex, C. Risko, R. S. Khnayzer, S. Barlow, D. Patra, T. V. Timofeeva, E. J. W. List, J. L. Bredas and S. R. Marder, *J. Mater. Chem. C*, 2013, **1**, 1638-1650.
12. H.-M. Wang, S.-H. Hsiao, G.-S. Liou and C.-H. Sun, *J. Polym. Sci., Part A: Polym. Chem.*, 2010, **48**, 4775-4789.
13. M. Banerjee, V. S. Vyas, S. V. Lindeman and R. Rathore, *Chem. Commun.*, 2008, 1889-1891.
14. A. Endo, K. Sato, K. Yoshimura, T. Kai, A. Kawada, H. Miyazaki and C. Adachi, *Appl. Phys. Lett.*, 2011, **98**, 083302.
15. G. Valchanov, A. Ivanova, A. Tadjer, D. Chercka and M. Baumgarten, *Org. Electron.*, 2013, **14**, 2727-2736.
16. D. N. Coventry, A. S. Batsanov, A. E. Goeta, J. A. K. Howard, T. B. Marder and R. N. Perutz, *Chem. Commun.*, 2005, **16**, 2172-2174.
17. A. G. Crawford, Z. Liu, I. A. I. Mkhaliid, M.-H. Thibault, N. Schwarz, G. Alcaraz, A. Steffen, J. C. Collings, A. S. Batsanov, J. A. K. Howard and T. B. Marder, *Chem. Eur. J.*, 2012, **18**, 5022-5035.
18. S. Shitagaki, S. Seo and R. Nomura, Google Patents, 2012.
19. S.-i. Kawano, M. Baumgarten, D. Chercka, V. Enkelmann and K. Müllen, *Chem. Commun.*, 2013, **49**, 5058-5060.
20. A. G. Crawford, A. D. Dwyer, Z. Liu, A. Steffen, A. Beeby, L.-O. Pålsson, D. J. Tozer and T. B. Marder, *J. Am. Chem. Soc.*, 2011, **133**, 13349-13362.
21. C. Reichardt and T. Welton, in *Solvents and Solvent Effects in Organic Chemistry*, Wiley-VCH Verlag GmbH & Co. KGaA, 2010, pp. 359-424.
22. S. O. Jeon, S. E. Jang, H. S. Son and J. Y. Lee, *Adv. Mater.*, 2011, **23**, 1436-1441.
23. S. Lee, S.-O. Kim, H. Shin, H.-J. Yun, K. Yang, S.-K. Kwon, J.-J. Kim and Y.-H. Kim, *J. Am. Chem. Soc.*, 2013, **135**, 14321-14328.
24. S.-J. Yoo, J.-H. Chang, J.-H. Lee, C.-K. Moon, C.-I. Wu and J.-J. Kim, *Sci. Rep.*, 2014, **4**.



A 2,7-functionalized pyrene-based emitter for highly efficient OLEDs has been developed. It offers an exceptional deep blue photoluminescence (CIE: $x = 0.16$, $y = 0.024$) and good external quantum efficiency (EQE) of 3.1 % when employed in a guest-host system OLED.